Design Study of Photonic Band Gap Structures for Axion Detection

Jara Wilensky, Harvard University — SULI Internship

FERMILAB-POSTER-22-172-AD-STUDENT

Abstract

Using Ansys High Frequency Structure Simulator, different designs of photonic band gap structures can be compared with the goal of designing a cavity that maximizes the signal power and scan rate for axion detection. This study focuses on the quality value and form factor of the cavity for the TM_{020} mode. Hexagonal lattices of different arrangements of sapphire and copper rods with radius to spacing ratios of 0.25 and 0.35 were simulated. Our figure of merit for the cavities was C^2Q.[1]

Introduction

As candidates for dark matter, axions must be detected indirectly through a photon resulting from an inverse Primakoff conversion.[2] The axion enters a magnetic field that is polarized along the length of a cavity, resulting in the conversion to a real photon that can be detected. The predicted axion mass range corresponds to frequencies up to hundreds of GHz for the resulting photon, necessitating cavity designs that boost signal power and support frequencies throughout a large range.

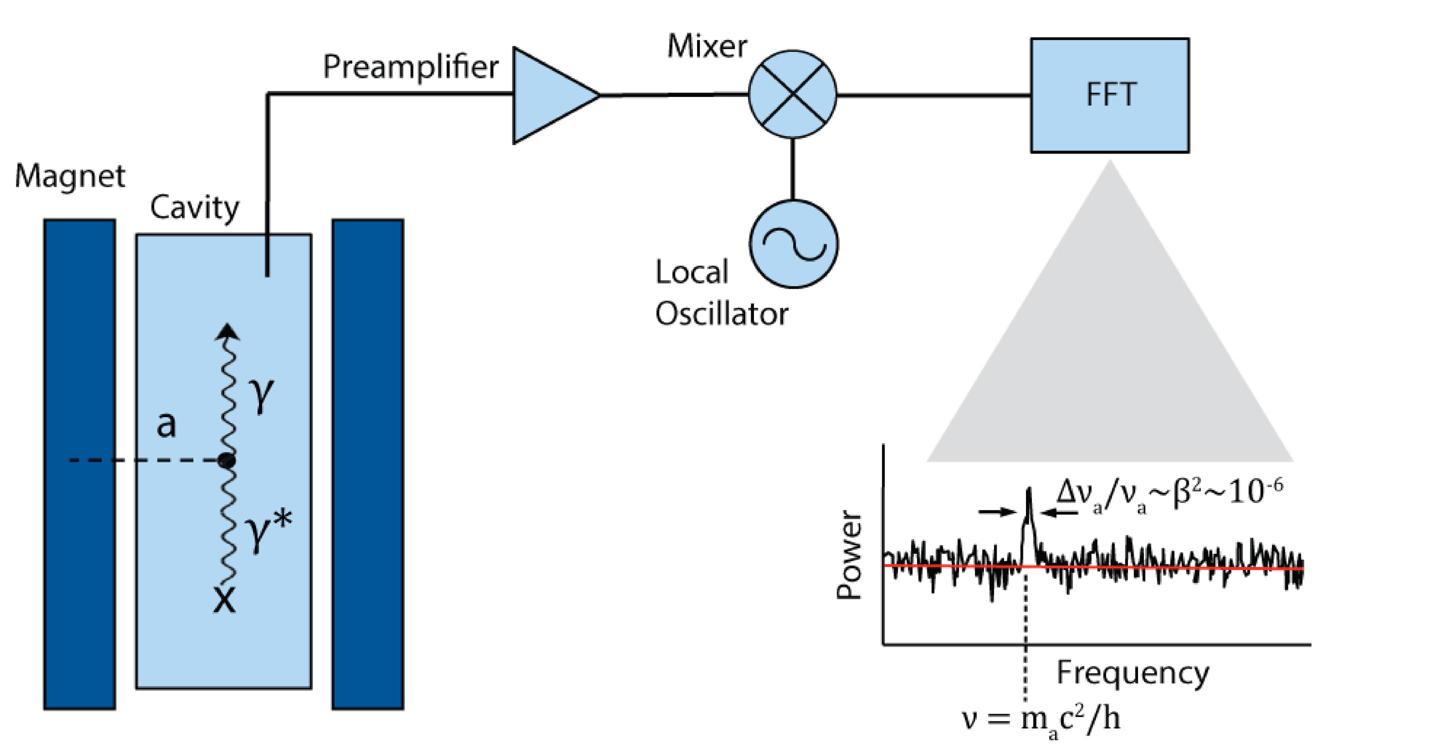

Figure 1: Cylindrical cavity. The axion enters the applied magnetic field and is converted into a photon. The frequency of the photon depends on the axion mass. [3]

Motivation

$$P \propto B_0^2 V Q_L C_{nm\ell} g_{a\gamma\gamma}^2$$

- Scan rate of searching different frequencies depends on the signal power to noise ratio and scales as V^2C^2Q [4]
- Increasing Q, the quality factor, and C, the form factor, can be done through cavity design
- C quantifies the amount of the E field aligned with the applied B field in the cavity and is maximized for the TM_{0n0} modes, with TM_{010} being the maximum
- Confining higher modes in the cavity allows higher frequencies to be searched, but lowers C
- Higher frequencies achieved through decreasing volume is impractical for tuning and lowers the scan rate
- Mode crossings between the TM_{0n0} modes and other modes can limit the tuning range

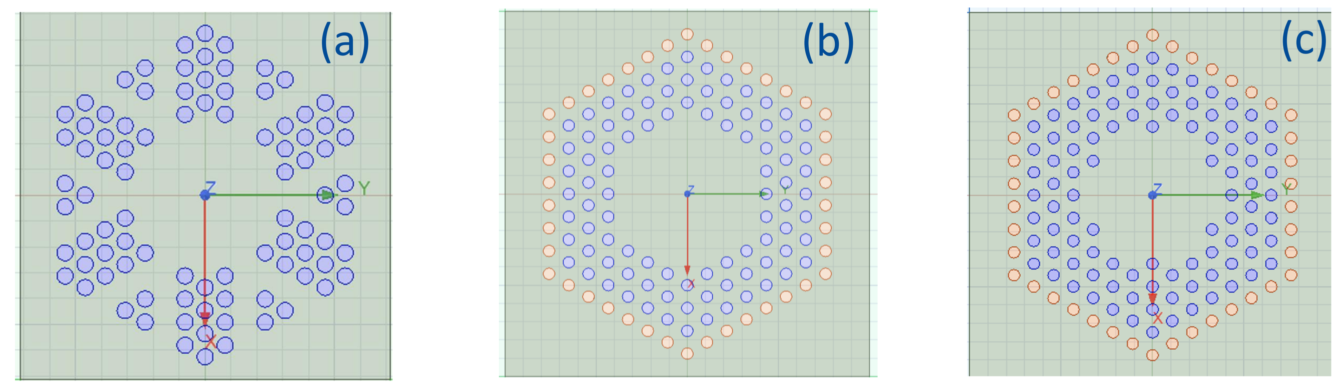

Figure 2: (a) Exit channels used to improve the Q value. (b) A row of copper added to the outside to improve confinement. (c) Additional sapphire rods placed at the vertices of the defect to improve shaping.

Photonic Band Gap Structures

- Lattices of dielectric rods have band gaps of disallowed frequencies
- Defects in the lattice can confine these frequencies while allowing others to freely propagate away
- Using low-loss dielectric materials allows for higher Q values without sacrificing the form factor
- By counteracting a lower form factor, we can search for higher order modes without lowering the signal power
- The frequency of the desired modes can be changed by modifying a/b, where a is the rod radius and b is the spacing between the rods

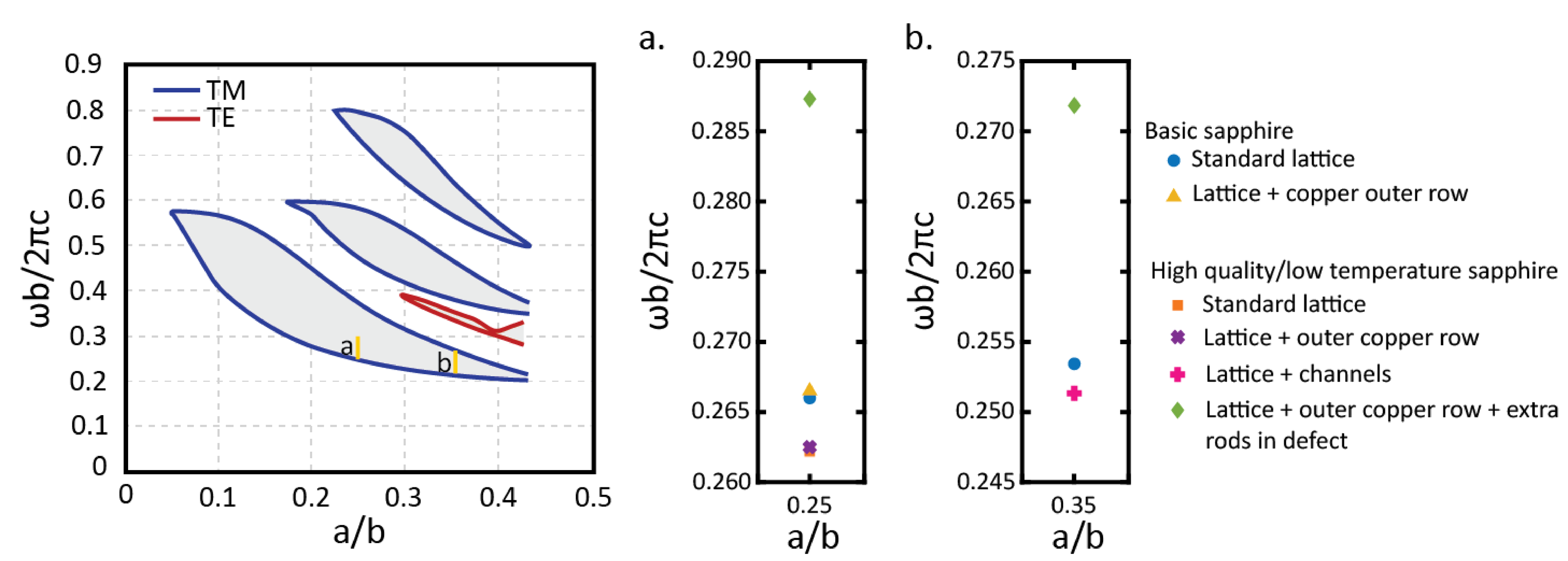

	Cylindrical	Standard	Channels	Outer Copper Row	Rods + Outer Copper
Freq. (GHz)	12.3932	12.3882	12.217	12.4019	13.5735
Q	22909.8	512.567	7875.22	1.45×10^6	1.72×10^7
C	0.1313	0.01057	0.007718	0.008751	0.009037
C^2Q	395.02	0.057295	0.46914	110.69	1406.6

	Cylindrical	Standard	Channels	Outer Copper Row	Rods + Outer Copper
Freq. (GHz)	16.7457	16.7572	16.6199	16.4566	17.9768
Q	26216.2	151.1	4999.23	6.67×10^5	3.38×10^7
C	0.1313	0.01262	0.008859	0.008419	0.006993
C^2Q	452.42	0.024074	0.39242	47.261	1655.1

Figure 3: The locations of the TM_{020} modes for different structure designs, material quality, and a/b plotted on the band gap map for the all-sapphire hexagonal lattice used to predict the mode frequencies. Where $a = 0.0625$in and a shortened cavity of length 1mm was simulated. [5]

Table: Above: A comparison of the cavity parameters for different designs for $a/b = 0.25$. "Outer Copper Row" refers to figure 2-b and "Rods + Outer Copper" refers to figure 2-c. The radius of the cylindrical cavity is calculated for a TM_{020} mode for a comparable frequency. Below: A comparison of the cavity parameters for different designs for $a/b = 0.35$. "Channels" refers to figure 2-a.

Results

Our figure of merit for the cavities, C^2Q, was greatest for the lattice designs with both an outer row of copper and rods at the vertices of the defect (figure 2-c). Changing a/b from 0.25 to 0.35 did not reliably increase or decrease our figure of merit. Other designs simulated include a full outer row of rods on the design with channels and replacing this outer row with copper (the design shown in figure 2-b with the addition of channels). For the former, no TM_{020} was found; for the latter, a TM_{020} mode was found at a frequency of 12.2187 GHz, $Q = 3.5 \times 10^6$, $C = 0.008382$. While the TM_{020} modes were used to determine the most successful design, TM_{030} modes were found for many of the PBG designs. These modes were found near 20 GHz and 27 GHz for .25 and .35 spacing, respectively. Their Q values were one to three orders of magnitude lower and their C at least one order of magnitude lower. For the majority of PBG designs simulated, the TM_{010} mode was not confined. For the outer copper row design, a possible TM_{010} mode was confined but had a C^2Q less than that of the initial cylindrical cavity. Overall, the use of certain PBG structures improves the scan rate, which scales as C^2Q, and signal power significantly for higher order modes compared to those of a cylindrical cavity, allowing for a higher possible range of masses for axions to be searched more quickly.

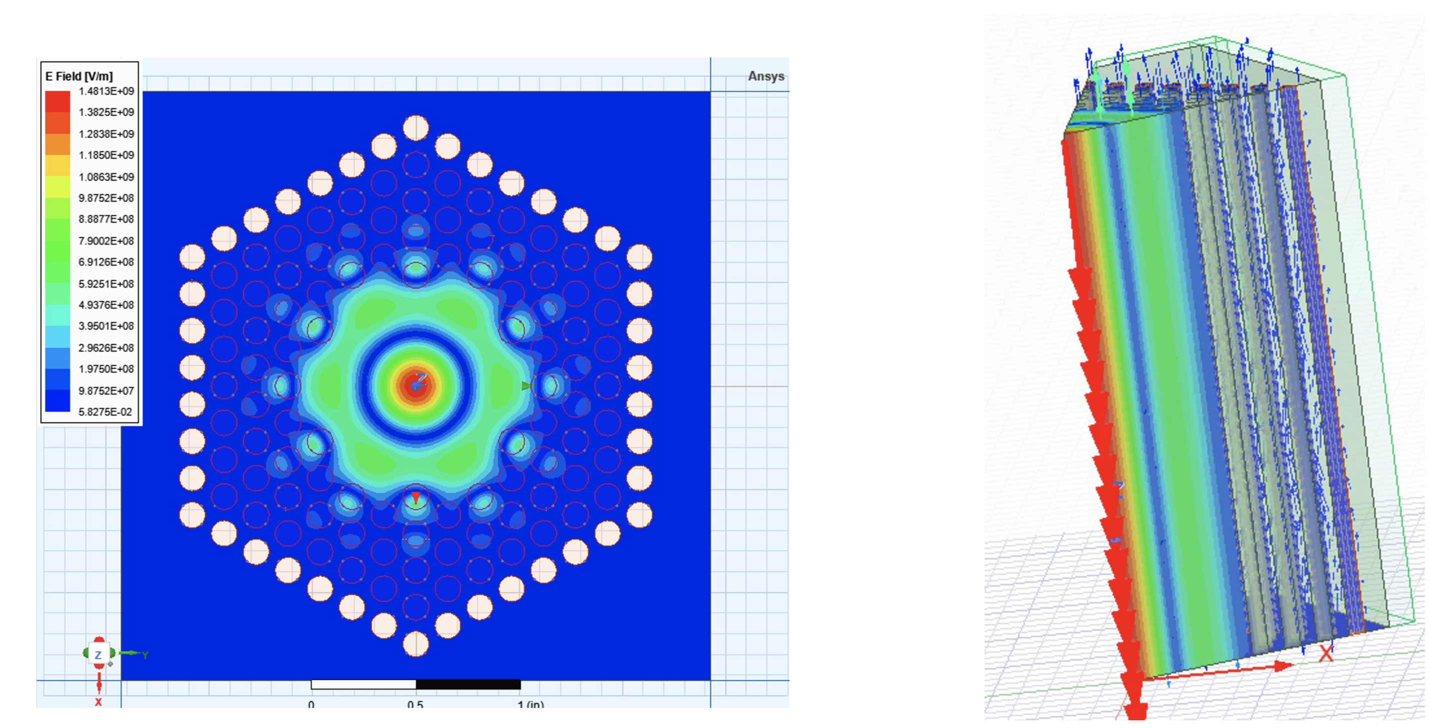

Figure 5: A 2D view of the TM_{020} mode for a 1mm tall design with an outer row of copper and rods at the vertices of the defect and a 100mm cavity cross-section of the mode showing the mode is the TM_{020} mode as the E field vectors are all in the direction of the length of the cavity. Simulating the shortened cavity lengths decreased the time needed to run and had no significant effect on the Q or C.

Acknowledgements

Thank you to my mentor Dr. Samantha Lewis for providing me with an ever-growing list of resources and patiently explaining each of them, as well as being an overall great mentor for my first research experience with high energy physics.

This manuscript has been authored by Fermi Research Alliance, LLC under Contract No. DE-AC02-07CH11359 with the U.S. Department of Energy, Office of Science, Office of High Energy Physics.

References: [1] Simanovskaia, M., Diss. UC Berkeley (2020). [2] Sikivie, P., *Phys Rev Lett* **51**, 16 (1983). [3] Lewis, S.M., Springer Proceedings in Physics, vol 211 (2018). [4] Rapidis, N.M., Review of Scientific Instruments **90,** 024706 (2019). [5] Zhang, J., Diss. Massachusetts Institute of Technology, (2016).